analytical chemistry

Article

pubs.acs.org/ac

Colorimetric Detection of Urine Glucose Based $ZnFe_2O_4$ Magnetic Nanoparticles

Li Su,[†,‡] Jie Feng,[†,‡] Ximin Zhou,[†,‡] Cuiling Ren,[†,‡] Honghong Li,[†,‡] and Xingguo Chen*[,†,‡,§]

[†]State Key Laboratory of Applied Organic Chemistry, Lanzhou University, Lanzhou 730000, China

[‡]Department of Chemistry, Lanzhou University, Lanzhou 730000, China

[§]Key Laboratory of Nonferrous Metal Chemistry and Resources Utilization of Gansu Province, Lanzhou 730000, China

Supporting Information

ABSTRACT: In this paper, we discovered that $ZnFe_2O_4$ magnetic nanoparticles (MNPs) possess intrinsic peroxidase-like activity. $ZnFe_2O_4$ MNPs exhibit several advantages such as high catalytic efficiency, good stability, monodispersion, and rapid separation over other peroxidase nanomimetics and horseradish peroxidase (HRP). $ZnFe_2O_4$ MNPs were used as a colorimetric biosensor for the detection of urine glucose. This method is simple, inexpensive, highly sensitive, and selective for glucose detection using glucose oxidase (GOx) and $ZnFe_2O_4$ MNPs with a linear range from 1.25×10^{-6} to 1.875×10^{-5} mol L^{-1} with a detection limit of 3.0×10^{-7} mol L^{-1}. The color change observable by the naked eyes based on the oxidation of 3,3′,5,5′-tetramethylbenzidine (TMB) is the principle for the sensing of urine glucose level.

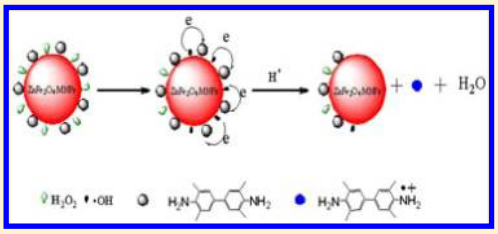

Colorimetric biosensing has attracted much attention because of its low cost, simplicity, and practicality. The key challenge for colorimetric biosensing is transforming the detection events into color changes. Since color changes can be read by the naked eye, colorimetric biosensing does not require expensive or sophisticated instrumentation and can be applied to field analysis and point-of-care diagnosis.[1−4] To this end, an enzyme-like nanomaterials based biosensor has emerged as an important colorimetric tool for the detection of biomolecules. Recently, it was reported first that Fe_3O_4 magnetic nanoparticles (MNPs) possessed intrinsic peroxidase-like activity,[5] and some metal oxide nanomaterials, such as CeO_2 NPs,[6] CuO NPs,[7] Co_3O_4 NPs,[8] and V_2O_5 nanowires,[9] were also found to possess intrinsic peroxidase-like activity. Besides metal oxide nanomaterials, carbon nanomaterials including single-wall,[10] helical carbon nanotubes,[11] graphene oxide,[12] carbon nanodots,[13] and multicolor luminescent carbon nanoparticles[14] displayed intrinsic enzyme mimetic activity. These enzyme-like nanomaterials could be employed to detect immunoassay,[5,6] nucleotide,[10] H_2O_2,[12,15] glucose,[12,15] melamine,[16] and so on. Subsequently, Hemin-Graphene hybrid nanosheets[17] and copper-creatinine complex[18] as multifunctional nanomaterials were used in the detection of DNA due to their intrinsic peroxidase-like activity. These enzyme-like nanomaterials were more stable against denaturation or protease digestion than horseradish peroxidase (HRP). Furthermore, their preparation and storage were relatively simple.

However, the application of some nanomaterials was restricted due to difficult separation and instability. It is therefore crucial to look for stable, separated easily, and high catalytic activity artificial enzyme mimetics from the viewpoint of practical application. Recently, Huang and co-workers reported that $CoFe_2O_4$ MNPs exhibited significant peroxidase-like activity,[19] and $CoFe_2O_4$ MNPs were more stable with exposure to air and could be separated by a magnet. However, the dispersibility of $CoFe_2O_4$ MNPs is poor. $CoFe_2O_4$ MNPs can be dispersed in solution through the functionalization of $CoFe_2O_4$ MNPs with chitosan polymers,[20] which leads to the complicated procedure of preparation. Therefore, the stable, dispersive, and easily separated nanomaterials as peroxidase mimetics with good catalytic properties and wide range of practical applications are becoming a significant field.

Diabetes mellitus is one of the most common noncommunicable diseases globally, and its related complications result in increasing disability, reduced life expectancy, and enormous health costs for virtually every society.[21] Therefore, the efforts to develop various sensors for fast and reliable monitoring glucose for the diagnosis of diabetes have received continuous interest.[22] The glucose level in blood is used as a clinical indicator of diabetes. However, it is inconvenient and painful to draw blood intravenously or by hand pricking. The presence of glucose in urine is a more dangerous condition, as it is an indication of worsening of diabetes. When the urine test is positive, the amount of glucose is more than 50−100 mg/dL.[23] Considering its convenience, painlessness, and affordability, urine glucose monitoring should not be completely given up, especially in low-income regions.[24]

Herein, we report first that $ZnFe_2O_4$ MNPs, one of the spinel ferrite compounds, exhibit intrinsic peroxidase-like activity. In this paper, as a mimic peroxidase, $ZnFe_2O_4$ MNPs exhibited good catalytic properties, stability, dispersibility, and rapid separation compared to other peroxidase nanomimetics and

Received: April 6, 2012
Accepted: June 13, 2012
Published: June 13, 2012

   dx.doi.org/10.1021/ac300939z | *Anal. Chem.* 2012, 84, 5753−5758

HRP, and the $ZnFe_2O_4$ MNPs were also successfully used as peroxidase mimetics for colorimetric detection of urine glucose.

EXPERIMENTAL SECTION

Materials. H_2O_2 (30%), $ZnCl_2$, $FeCl_3·6H_2O$, ethylene glycol, polyethylene glycol, $NaCH_2COOH$ (NaAc), and CH_3COOH (HAc) were purchased from Tianjin Guangfu Chemical Reagent Factory (Tianjin, China). Hydroxylamine hydrochloride was purchased from Sinopharm Chemical Reagent Co., Ltd. (Shanghai, China). Glucose was purchased from Sangon Biotech (Shanghai) Co. Ltd. Glucose oxidase (GOx, 50 KU) was purchased from Sigma-Aldrich and stored in a refrigerator at −18 °C. 3,3′,5,5′-Tetramethylbenzidine (TMB) was purchased from Sigma-Aldrich. Fructose, lactose, maltose, and 1,10-phenanthroline monohydrate were purchased from Shanghai Zhongqin Chemical Reagent Company (Shanghai, China). The urine sample was obtained from a male volunteer with diabetes. All other chemicals were of analytical reagent grade and used without further purification. Deionized water was used throughout the experiment.

Apparatus and Characterization. A TU-1901 double beam UV−vis spectrophotometer (Beijing Purkine General Instrument Co. Ltd., China) was used to implement kinetic experiments and scan spectrum. A Vis-7220 Spectrophotometer (Beijing Rayleigh Analysis Instrument Co. China) was used to measure absorbance. A Hitachi-600 transmission electron microscope (TEM) was used for measuring the morphologies and size of $ZnFe_2O_4$ MNPs. An X-ray diffraction (XRD) pattern of $ZnFe_2O_4$ MNPs was carried out with a X'Pertpro Philips X-ray diffractometer with Cu Kα radiation (λ = 0.154056). A magnetic hysteresis loop of the prepared $ZnFe_2O_4$ MNPs was carried out with a vibration sample magnetometer (VSM, Lakeshore cryotronics 730, USA) at room temperature. Zeta potential measurements of $ZnFe_2O_4$ MNPs were performed with a Malvern Nano-ZS apparatus. Fluorometric measurement was carried out by a RF-5301PC spectrofluorophotometer (Shimadzu).

Preparation of $ZnFe_2O_4$ Magnetic Nanoparticles. $ZnFe_2O_4$ MNPs were prepared using a hydrothermal method as described elsewhere.[25] Briefly, $ZnCl_2$ (0.34 g, 2.5 mmol) and $FeCl_3·6H_2O$ (1.35 g, 5 mmol) were dissolved in ethylene glycol (40 mL) to form a clear solution, followed by the addition of NaAc (3.6 g) and polyethylene glycol 20 000 (1.0 g). The mixture was stirred vigorously for 30 min and then sealed in a teflonlined stainless-steel autoclave (50 mL capacity). The autoclave was heated to and maintained at 200 °C for 8 h and allowed to cool to room temperature. The black products were washed several times with ethanol and dried at 60 °C for 6 h.

Detection of Iron Ions Leached from the $ZnFe_2O_4$ MNPs in the Buffer Solutions of Different pH. Five hundred microliters of 1.0 g mL^{-1} hydroxylamine hydrochloride was added into 500 μL of the supernatant of 5 mg mL^{-1} $ZnFe_2O_4$ solution, and 100 μL of 1.5 mg mL^{-1} 1,10-phenanthroline monohydrate was added into the above mixing solution; then, the solution color rapidly turned to orange. The absorbance of the mixing solution was measured at 508 nm.

Preparation of Urine Sample. For glucose determination in urine from a male diabetic, the collected sample was stored at −18 °C and thawed at ambient temperature before further preparation. First, the sample was centrifuged at 12 000 rpm for 40 min, and then, the supernatant was diluted 15 times using NaH_2PO_4 buffer (0.5 mM, pH 7.0) before measurement.

Detection of Urine Glucose Using $ZnFe_2O_4$ MNPs and GOx. Urine glucose detection was performed as follows: (a) 10 μL of 1 mg mL^{-1} GOx and 45 μL of urine sample in 0.5 mM Na_2HPO_4 buffer (pH 7.0) were incubated at 37 °C for 30 min; (b) 55 μL of 20 mM TMB, 20 μL of 5 mg mL^{-1} $ZnFe_2O_4$ MNPs, and 470 μL of 0.2 M HAc-NaAc buffer (pH 4.0) were added into the above 55 μL glucose reaction, and the pH of the final resulting solution was 4.0; (c) the mixed solution was incubated at 40 °C for 10 min and then kept in an ice−water bath for 10 min to terminate the reaction; (d) the $ZnFe_2O_4$ MNPs were then removed from the reaction solution by an external magnetic field; (e) 500 μL of the resulting solution without $ZnFe_2O_4$ MNPs was added into 2.5 mL of deionized water in a 10 mL cuvette; then, the solution was mixed up to make it uniform and used for absorbance measurement at a wavelength of 652 nm.

RESULTS AND DISCUSSION

Characterization of $ZnFe_2O_4$ MNPs. The as-prepared $ZnFe_2O_4$ MNPs were identified from the X-ray diffraction (XRD) patterns (Figure S1a, Supporting Information) with a suitable spinel structure (JCPDS 22-1012). Transmission electron microscopy (TEM) (Figure S2, Supporting Information) revealed that $ZnFe_2O_4$ MNPs were spherical and dispersive with an average size of about 200 nm. The magnetic property of $ZnFe_2O_4$ MNPs was investigated at 298 K using a vibrating sample magnetometer (VSM). Figure S3 (Supporting Information) showed that the magnetization hysteresis loops appeared S-like and the saturation magnetization was 65 $emu·g^{-1}$. Figure S4 (Supporting Information) showed the variation of zeta potential of $ZnFe_2O_4$ MNPs with equilibrium pH. The obtained zeta potential value of $ZnFe_2O_4$ MNPs decreased with the increase of pH, and the isoelectrical point (IEP) was about 4.8. The value of zeta potential is 4.92 mV at pH 4.0, suggesting the surface of $ZnFe_2O_4$ MNPs has positive charge at the pH.

Peroxidase-Like Activity of $ZnFe_2O_4$ MNPs. The catalysis of peroxidase substrate 3,3′,5,5′-tetramethylbenzidine (TMB) was tested in the presence of H_2O_2. $ZnFe_2O_4$ MNPs were added into the peroxidase substrate TMB in the presence of H_2O_2. As shown in Figure 1, the $ZnFe_2O_4$ MNPs could catalyze the oxidation of TMB by H_2O_2 to produce the typical blue color reaction. The maximum absorbance of the reaction

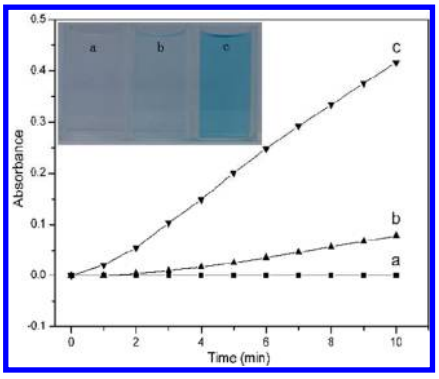

Figure 1. Time-dependent absorbance changes at 652 nm of TMB in different reaction systems: (a) $ZnFe_2O_4$ MNPs + TMB, (b) TMB + H_2O_2, and (c) TMB + $ZnFe_2O_4$ MNPs + H_2O_2 in a pH 4.0 HAc-NaAc buffer (0.2 M) at 40 °C. Inset shows the color change of different samples.

dx.doi.org/10.1021/ac300939z | Anal. Chem. 2012, 84, 5753−5758

mixture was 652 nm, which originated from the oxidation of TMB. Additional control experiments showed that the absorbance of the $ZnFe_2O_4$ MNPs-TMB-H_2O_2 system was much higher than that of the TMB-H_2O_2 system, and the $ZnFe_2O_4$ MNPs-TMB system had no absorbance in 652 nm. It indicated that both the components were required for the reaction, as was also the case for horseradish peroxidase (HRP). The composition and phase of $ZnFe_2O_4$ MNPs after the peroxidase reaction 10 times remained unchanged (Figure S1, Supporting Information). The results confirmed that $ZnFe_2O_4$ MNPs exhibit an intrinsic peroxidase-like activity. To further characterize the peroxidase-like activity of the $ZnFe_2O_4$ MNPs, other typical peroxidase substrates were used in place of TMB, including 2,2-azino-bis(3-ethylbenzothiazoline-6-sulfonic acid) (ABTS) and *o*-phenylenediamine (OPD). The oxidation of ABTS and OPD catalyzed by the $ZnFe_2O_4$ MNPs formed more green and orange product, respectively (Figure 2).

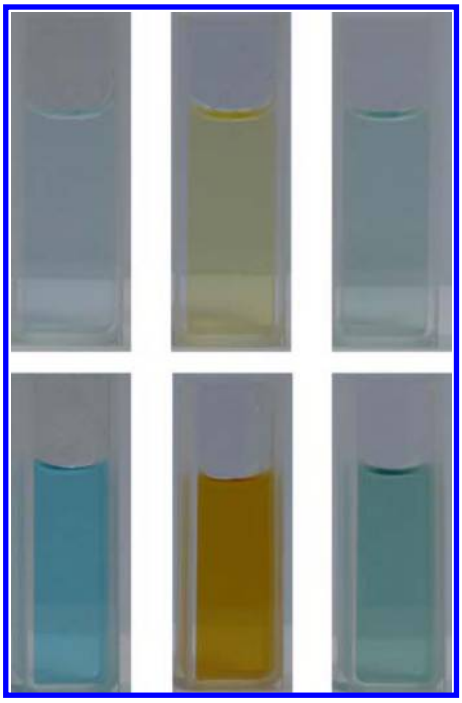

Figure 2. Images of oxidation color reaction of TMB, OPD, and ABTS by H_2O_2 (from left to right) before (above) and after (below) by the catalysis of $ZnFe_2O_4$ MNPs.

It is important to rule out the possibility that the observed activity was caused by $ZnFe_2O_4$ MNPs rather than iron ions leaching from $ZnFe_2O_4$ MNPs in acidic solution. To test this, $ZnFe_2O_4$ MNPs were incubated in the reaction buffer (pH 4.0) for 2 h and then removed from solution by an external magnetic field. As shown in Figure 3, comparing the activity of the leaching solution with that of $ZnFe_2O_4$ MNPs under the same conditions, the leaching solution had no activity, showing that the observed peroxidase-like activity was due to intact $ZnFe_2O_4$ MNPs.

Optimization of Experimental Conditions. Similar to NPs based peroxidase mimetics and HRP, the catalytic activity of $ZnFe_2O_4$ MNPs is also dependent on pH, temperature, and H_2O_2 concentration. The catalytic activity was much higher in acidic solutions than in neutral and basic solutions (Figure S5a, Supporting Information). However, the iron ions could be leached from the $ZnFe_2O_4$ MNPs in the buffer solutions of pH

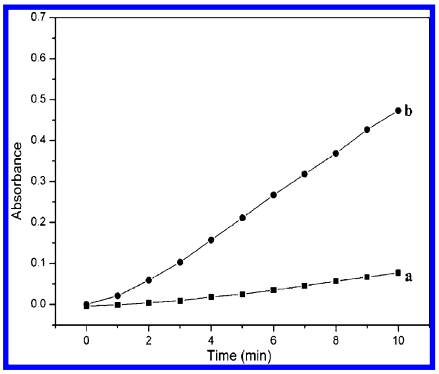

Figure 3. Time-dependent absorbance evolution of TMB oxidation system at 652 nm in the presence of $ZnFe_2O_4$ MNPs (a) and leaching solution (b).

< 4.0. In order to prove the phenomenon, the concentration of iron ions in the supernatant of $ZnFe_2O_4$ solution was detected using the colorimetric method.[26] From Figure S6, Supporting Information, the absorbance of the supernatants of $ZnFe_2O_4$ MNPs solution at pH ≥ 4.0 can be ignored at 508 nm, which suggested that the iron ions leached scarcely from the $ZnFe_2O_4$ MNPs. In view of the stability and catalytic activity of the $ZnFe_2O_4$ MNPs, 4.0 was set as the optimal pH value. The optimal temperature and H_2O_2 concentration were 40 °C and 500 mM, respectively (Figure S5b,c, Supporting Information).

Steady-State Kinetic Assay of $ZnFe_2O_4$ MNPs. To investigate the kinetic mechanism of the peroxidase-like activity of $ZnFe_2O_4$ MNPs, apparent steady-state kinetic parameters for the peroxidase-like color reaction were determined by changing the concentration of TMB and H_2O_2 in this system, respectively. Kinetic experiments were carried out at 40 °C using 40 μg mL^{-1} $ZnFe_2O_4$ MNPs in a reaction volume of 3.0 mL of HAc-NaAc buffer solution (0.2 M, pH 4.5) with 320 μM TMB as substrate, and the H_2O_2 concentration was 0.2 mM, unless otherwise stated. Typical Michaelis−Menten curves were obtained with both TMB and H_2O_2 by monitoring the absorbance change at 652 nm for 5 min (Figure S7a,b, Supporting Information). Michaelis−Menten constant (K_m) and maximum initial velocity (V_{max}) were obtained using Lineweaver−Burk plot (Table 1).[5] The smaller the value of K_m, the stronger is the affinity between the enzyme and the substrate. The apparent K_m value for the $ZnFe_2O_4$ MNPs with H_2O_2 as the substrate was lower than HRP (Table 1), suggesting that the $ZnFe_2O_4$ MNPs had higher affinity for H_2O_2 than HRP. The apparent K_m value of the $ZnFe_2O_4$ MNPs with TMB was larger than that of HRP, suggesting that the $ZnFe_2O_4$ MNPs had a lower affinity for TMB than HRP. The larger size of $ZnFe_2O_4$ MNPs (about 200 nm) may be due to the lower affinity of TMB to $ZnFe_2O_4$ MNPs. The transformation constant (K_{cat}) is equal to $V_{max}/[E]_0$, where $[E]_0$ is overall enzyme concentration (both bound and unbound). The greater the value of K_{cat}, the higher is the enzymatic activity. The K_{cat} value of the $ZnFe_2O_4$ MNPs with TMB as the substrate was 4.36×10^{10} s^{-1}, which was 175 and 5×10^5 times larger than that of CGN and Fe_3O_4 MNPs, respectively (Table 1). To date, the catalytic activity of $ZnFe_2O_4$ MNPs was higher than the reported literature.[5,8,27] To further investigate the mechanism of the catalysis of $ZnFe_2O_4$ MNPs, we measured their activity under standard reaction condition by varying concentration of TMB at a fixed concentration of H_2O_2 or vice versa. The double reciprocal plots of initial velocity against the

dx.doi.org/10.1021/ac300939z | *Anal. Chem.* 2012, 84, 5753−5758

Table 1. Comparison of the Kinetic Parameters of the Oxidation Reaction Catalyzed by the $ZnFe_2O_4$ MNPs and Reported Fe_3O_4 MNPs, Co_3O_4 NPs, CGN, and HRP

catalyst	substance	$[E]_0$/M	K_m/mM	$V_{max}/10^{-8}$ M·s^{-1}	K_{cat}/s^{-1}
HRP[5]	TMB	2.5×10^{-11}	0.434	10	4.00×10^3
	H_2O_2	2.5×10^{-11}	3.7	8.71	3.48×10^3
Fe_3O_4 MNPs[5]	TMB	11.4×10^{-13}	0.098	3.44	8.58×10^4
	H_2O_2	11.4×10^{-13}	154	9.78	3.02×10^4
Co_3O_4 NPs[8]	TMB	3.43×10^{-10}	0.037	6.27	1.83×10^2
	H_2O_2	3.43×10^{-10}	140.07	12.1	3.53×10^2
CGN[26]	TMB	$>1.34 \times 10^{-15}$	0.12	33.2	2.48×10^8
	H_2O_2	$>1.34 \times 10^{-15}$	245	28.5	2.13×10^8
$ZnFe_2O_4$ MNPs	TMB	3.05×10^{-18}	0.85	13.31	4.36×10^{10}
	H_2O_2	3.05×10^{-18}	1.66	7.74	2.54×10^{10}

concentration of one substrate were obtained over a range of concentrations of the second substrate (Figure S7c,d, Supporting Information). The slopes of the lines were parallel, which was characteristic of a ping-pong mechanism, as observed for HPR.[5] This indicated that $ZnFe_2O_4$ MNPs bind and react with the first substrate and then release the first product before reacting with the second substrate. This product may be hydroxyl radical (·OH), which originated from the decomposition of H_2O_2 due to the catalysis of $ZnFe_2O_4$ MNPs.

Mechanism of Peroxidase-Like Activity of $ZnFe_2O_4$ MNPs. To evidence this assumption, the ·OH formation was assessed by adding the fluorescent probe terephthalic acid into the H_2O_2-$ZnFe_2O_4$ MNPs system, where terephthalic acid easily reacted with ·OH to form highly fluorescent 2-hydroxy terephthalic acid.[28] The procedure of experiment was carried out using 50 mM H_2O_2, 0.625 mM terephthalic acid, and different concentrations of the $ZnFe_2O_4$ MNPs incubating in 0.2 mM HAc-NaAc buffer (pH 4.0) at 40 °C for 8 h. It was clearly shown that gradual increase of the fluorescence intensity was observed as the concentration of the $ZnFe_2O_4$ MNPs increased, suggesting that the amount of generated ·OH was increased by the increase in $ZnFe_2O_4$ MNPs. However, there was no fluoresence intensity in the absence of H_2O_2 (Figure 4). These results indicated that $ZnFe_2O_4$ MNPs could decompose H_2O_2 to generate the ·OH radical.

A possible catalytic mechanism of $ZnFe_2O_4$ MNPs was presented in Scheme 1; i.e., first, H_2O_2 molecules were adsorbed on the surface of $ZnFe_2O_4$ MNPs and then activated

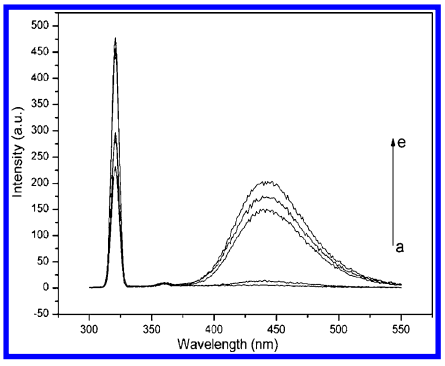

Figure 4. The effect of the $ZnFe_2O_4$ MNPs on the formation of hydroxyl radical with terephthalic acid as a fluorescence probe. (a) 1/3 mg mL^{-1} $ZnFe_2O_4$ MNPs, without H_2O_2; (b–e) 0, 1/3, 2/3, and 1 mg mL^{-1} $ZnFe_2O_4$ MNPs, 50 mM H_2O_2. Reaction conditions: 0.625 mM terephthalic acid and different solutions were incubated in 0.2 mM HAc-NaAc buffer (pH 4.0) at 40 °C for 8 h.

Scheme 1. Possible Mechanism for the $ZnFe_2O_4$ MNPs-H_2O_2-TMB System

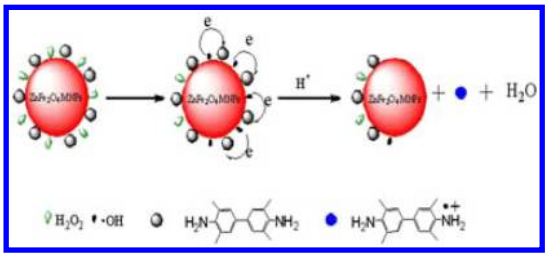

by the bound Fe^{3+} to generate the ·OH, and the generated ·OH was stabilized by $ZnFe_2O_4$ MNPs via partial electron exchange interaction.[19] Second, TMB was oxidized by ·OH to form a blue color product. The blue signal comes from the charge-transfer complex, consisting of a cation free radical and TMB.[29]

Robustness of Peroxidase Activity of $ZnFe_2O_4$ MNPs. The stability of the $ZnFe_2O_4$ MNPs in wide pH and temperature ranges is crucial to extend their applications. As inorganic materials, $ZnFe_2O_4$ MNPs were expected to be more stable than natural enzymes. As for HRP, after treatment at pH lower than 5.0 or temperatures greater than 40 °C for 2 h, the enzyme activity dramatically declines.[5] In contrast, $ZnFe_2O_4$ MNPs were stable when they were incubated at a wide range of pHs (2–11) and temperatures (0–90 °C) for 2 h (Figure S8a,b, Supporting Information). The robustness of $ZnFe_2O_4$ MNPs makes them suitable for a broad range of applications in the biomedicine and environmental chemistry fields.

Detection of Urine Glucose Using $ZnFe_2O_4$ MNPs. Since the catalytic activity of $ZnFe_2O_4$ MNPs is H_2O_2 concentration dependent and H_2O_2 is the main product of the glucose oxidase (GOx)-catalyzed reaction, a colorimetric detection of glucose could be realized using $ZnFe_2O_4$ MNPs instead of the traditional usage of HRP. Figure 5a showed typical glucose concentration–response curves. The linear range for glucose was from 1.25×10^{-6} to 1.875×10^{-5} mol L^{-1} with a detection limit (DL) of 3.0×10^{-7} mol L^{-1} (Figure 5b). This detection method based on $ZnFe_2O_4$ MNPs gave a lower DL than the method using Fe_3O_4 nanoparticles as catalyst (3×10^{-5} mol L^{-1}),[15] which was attributed to the presence of $ZnFe_2O_4$ MNPs. Using this method, we detect glucose in urine sample with diabetes from a male volunteer. Figure 6 showed the UV–vis spectra and the good colorimetric differentiation. From the UV–vis spectra, it is indicated that the method was largely free from the complicated sample matrix effect of the simple preparation of urine sample. According to the calibration curve, the concentration of glucose in urine was

dx.doi.org/10.1021/ac300939z | Anal. Chem. 2012, 84, 5753–5758

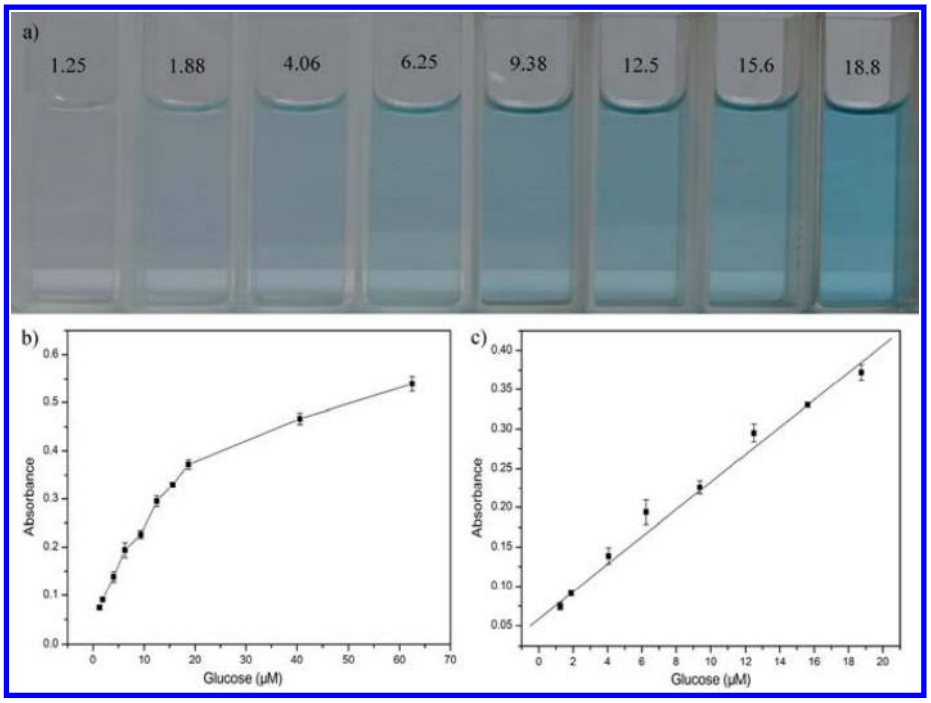

Figure 5. (a) The photograph of the colored products for different concentrations of glucose (μM). (b) A dose−response curve for glucose detection at 652 nm under the optimum conditions. (c) The linear calibration plot for glucose. The error bars represent the standard deviation of three measurements.

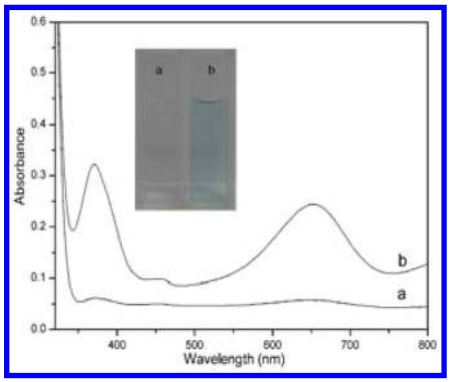

Figure 6. UV−vis spectra of buffer solution (a) and 15-fold serial dilution of urine sample (b). Inset: Images of production of colored product for buffer solution and urine sample.

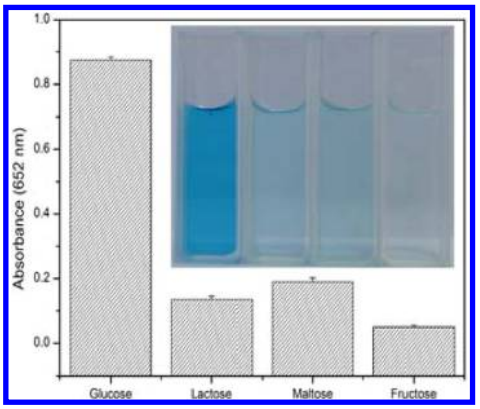

Figure 7. Determination of the selectivity of glucose detection (from left to right: 0.4 mM glucose, 2.0 mM maltose, 2.0 mM fructose, and 2.0 mM lactose). Inset: The color change with the different solutions. The error bars represent the standard deviation of three measurements.

10.6 mM (114.7 mg dL^{-1}). The urine test is positive when the amount of glucose is more than 50−100 mg dL^{-1}.[23] Therefore, this colorimetric method is applicable to urine sample to determine glucose concentration.

Selectivity of the Method. To test the selectivity of detection of glucose, the control experiments were taken using fructose, lactose, and maltose. The selectivity of the colorimetric method was shown in Figure 7. Even when the concentration of control samples was 5 times larger than glucose, the absorbance of glucose is higher than that of control samples. It shows that these compounds did not interfere with the determination of urine glucose.

CONCLUSION

In summary, we provide the first report that the $ZnFe_2O_4$ MNPs possess intrinsic peroxidase-like activity. As a novel mimic peroxidase, the $ZnFe_2O_4$ MNPs show several advantages over HRP and other peroxidase nanomimetics, such as stability, dispersibility, separability, and high catalytic efficiency. On the basis of this finding, we provide a simple, inexpensive, highly sensitive, and selective method for colorimetric detection of urine glucose. The method seems to be useful, particularly for the rural population in third world countries, and our work will facilitate the utilization of $ZnFe_2O_4$ MNPs intrinsic peroxidase-like activity in environmental chemistry, biotechnology, and medicine.

ASSOCIATED CONTENT

Supporting Information

Additional information as noted in text. This material is available free of charge via the Internet at http://pubs.acs.org.

dx.doi.org/10.1021/ac300939z | *Anal. Chem.* 2012, 84, 5753−5758

AUTHOR INFORMATION

Corresponding Author

*E-mail: chenxg@lzu.edu.cn.

Notes

The authors declare no competing financial interest.

ACKNOWLEDGMENTS

The authors are grateful for financial support from the National Natural Science Foundation of China (No. 20875040) and the Fundamental Research Funds for the Central Universities (No. zujbky-2011-28).

REFERENCES

(1) Stewart, M. E.; Anderton, C. R.; Thompson, L. B.; Maria, J.; Gray, S. K.; Rogers, J. A.; Nuzzo, R. G. *Chem. Rev.* **2008**, *108*, 494−521.

(2) De, M.; Ghosh, P. S.; Rotello, V. M. *Adv. Mater.* **2008**, *20*, 4225−4241.

(3) Liu, J.; Cao, Z.; Lu, Y. *Chem. Rev.* **2009**, *109*, 1948−1998.

(4) Song, S.; Qin, Y.; He, Y.; Huang, Q.; Fan, C.; Chen, H. Y. *Chem. Soc. Rev.* **2010**, *39*, 4234−4243.

(5) Gao, L. Z.; Zhuang, J.; Nie, L.; Zhang, J. B.; Zhang, Y.; Gu, N.; Wang, T. H.; Feng, J.; Yang, D. L.; Perrett, S.; Yan, X. *Nat. Nanotechnol.* **2007**, *2*, 577−583.

(6) Asati, A.; Santra, S.; Kaittanis, C.; Nath, S.; Perez, J. M. *Angew. Chem., Int. Ed.* **2009**, *48*, 2308−2312.

(7) Chen, W.; Chen, J.; Liu, A. L.; Wang, L. M.; Li, G. W.; Lin, X. H. *ChemCatChem* **2011**, *3*, 1151−1154.

(8) Mu, J.; Wang, Y.; Zhao, M.; Zhang, L. *Chem. Commun.* **2012**, *48*, 2540−2542.

(9) Andre, R.; Natalio, F.; Humanes, M.; Leppin, J.; Heinze, K.; Wever, R.; Schroeder, H. C.; Mueller, W. E. G.; Tremel, W. *Adv. Funct. Mater.* **2011**, *21*, 501−509.

(10) Song, Y. J.; Wang, X. H.; Zhao, C.; Qu, K. G.; Ren, J. S.; Qu, X. G. *Chem.−Eur. J.* **2010**, *16*, 3617−3621.

(11) Cui, R. J.; Han, Z. D.; Zhu, J. J. *Chem.−Eur. J.* **2011**, *17*, 9377−9384.

(12) Song, Y. J.; Qu, K. G.; Zhao, C.; Ren, J. S.; Qu, X. G. *Adv. Mater.* **2010**, *22*, 2206−2210.

(13) Shi, W. B.; Wang, Q. L.; Long, Y. J.; Cheng, Z. L.; Chen, S. H.; Zheng, H. Z.; Huang, Y. M. *Chem. Commun.* **2011**, *47*, 6695−6697.

(14) Wang, X. H.; Qu, K. G.; Xu, B. L.; Ren, J. S.; Qu, X. G. *Nano Res.* **2011**, *4*, 908−920.

(15) Wei, H.; Wang, E. *Anal. Chem.* **2008**, *80*, 2250−2254.

(16) Ding, N.; Yan, N.; Ren, C.; Chen, X. *Anal. Chem.* **2010**, *82*, 5897−5899.

(17) He, W.; Liu, Y.; Yuan, J.; Yin, J.-J.; Wu, X.; Hu, X.; Zhang, K.; Liu, J.; Chen, C.; Ji, Y.; Guo, Y. *Biomaterials* **2011**, *32*, 1139−1147.

(18) Singh, A.; Patra, S.; Lee, J. A.; Park, K. H.; Yang, H. *Biosens. Bioelectron.* **2011**, *26*, 4798−4803.

(19) Shi, W.; Zhang, X.; He, S.; Huang, Y. *Chem. Commun.* **2011**, *47*, 10785−10787.

(20) Fan, Y.; Huang, Y. *Analyst* **2012**, *137*, 1225−1231.

(21) Lu, J.; Bu, R. F.; Sun, Z. L.; Lu, Q. S.; Jin, H.; Wang, Y.; Wang, S. H.; Li, L.; Xie, Z. L.; Yang, B. Q. *Diabetes Res. Clin. Pract.* **2011**, *93*, 179−186.

(22) Reach, G.; Wilson, G. S. *Anal. Chem.* **1992**, *64*, 381A−386A.

(23) Urakami, T.; Suzuki, J.; Yoshida, A.; Saito, H.; Mugishima, H. *Diabetes Res. Clin. Pract.* **2008**, *80*, 473−476.

(24) Radhakumary, C.; Sreenivasan, K. *Anal. Chem.* **2011**, *83*, 2829−2833.

(25) Deng, H.; Li, X.; Peng, Q.; Wang, X.; Chen, J.; Li, Y. *Angew. Chem., Int. Ed.* **2005**, *117*, 2842−2845.

(26) Adhikamsetty, R.; Gollapalli, N.; Jonnalagadda, S. *Int. J. Chem. Kinet.* **2008**, *40*, 515−523.

(27) Yin, J.; Cao, H.; Lu, Y. *J. Mater. Chem.* **2011**, *22*, 527−534.

(28) Ishibashi, K.; Fujishima, A.; Watanabe, T.; Hashimoto, K. J. *Photochem. Photobiol., A* **2000**, *134*, 139−142.

(29) Gao, L.; Wu, J.; Gao, D. *ACS Nano* **2011**, *5*, 6736−6742.